

Third order viscous hydrodynamics from the entropy four current

Mohammed Younus ^{*}

Department of Physics, Nelson Mandela University, Port Elizabeth 6031, South Africa

Azwinndini Muronga [†]

Faculty of Science, Nelson Mandela University, Port Elizabeth 6031, South Africa

 (Received 6 December 2019; revised 11 June 2020; accepted 10 August 2020; published 3 September 2020)

Nonequilibrium dynamics for relativistic fluid or quark gluon plasma (QGP) have already been calculated earlier up to third order using both kinetic and thermodynamic approaches. Calculations presented in this article are based on thermodynamics principles. The expressions for third order dissipative fluxes have been derived from equation for entropy four-current developed earlier by Muronga. The relaxation equations in the present work have been developed in a simple Bjorken (1 + 1) dimensional scenario and Eckart frame. The relaxation equations are found to have slightly different values for the coupling coefficients as compared to calculations from earlier models. The solutions to the differential equations have been found to be sensitive to values of these coefficients. The shear relaxation equations derived in third order theory are discussed term by term. Effects of third order theory on shear relaxation time have been discussed. Thermodynamic quantities related to hot and dense matter have been calculated as functions of proper time. Moreover, various initial conditions for the relaxation equations have been assumed to study their effects on above mentioned observables. A CERN Large Hadron Collider QGP formation time of $\tau_0 = 0.4$ fm/c and temperature of $T_0 = 500$ MeV have been assumed.

DOI: [10.1103/PhysRevC.102.034902](https://doi.org/10.1103/PhysRevC.102.034902)

I. INTRODUCTION

High energy heavy ion collisions offer the opportunity to study the properties of hot and dense quark gluon plasma (QGP) [1]. At the CERN Large Hadron Collider (LHC), experimental results have suggested the formation of a relativistic fluid with observables on particle production and have thus confirmed the formation of QGP [2–4]. In order to study the system of relativistic fluid evolving through space and time, one must use transport equations. Transport equations do not merely transport particle distributions without any medium effects or particle interaction but also include various physical and nonequilibrium processes such as dissipations, collisions, and radiations. The nonequilibrium phenomena are particularly interesting because of the various transport coefficients and their relaxation times and length scales which may help us track the equilibration of the system. Thus the use of fluid dynamics as one of the approaches in modeling the dynamic evolution of nuclear collisions has been successful in describing many of the observables [5–7]. However the assumptions and the approximations of the fluid dynamical models have been the source of major uncertainties in predicting the observables.

Many works have been done earlier on relativistic fluid dynamics [8] both from kinetic theory and thermodynamics approaches. The first order theories of relativistic fluid dynamics are due to Eckart *et al.* [9], and to Landau and Lifshitz [10],

and had assumptions that the entropy four-current contains only linear terms in dissipative quantities. Consequently we have Fourier-Navier-Stokes equations which might lead to noncausality and propagate viscous and thermal signals with speed greater than that of light. These theories have been extended to include second order equations to meet the causality conditions and have been done at the earliest by Muller, Israel, and Stewart. This is also known as second order dissipative theories or Muller-Israel-Stewart theories (M-IS) [11–13]. Recent works to include second order corrections have been done by Muronga *et al.* [14–17], El *et al.* [18,19] using thermodynamics approaches (entropy principle), while Denicol *et al.* [20], Jaiswal *et al.* [21,22] used an iterative approach to the kinetic Boltzmann equation (BE) to solve the dissipative equations. The results from these various approaches are complimentary [23]. However their differences are considerable and depend on the approaches or techniques involved and values of the coefficients in the differential equations. We will return to this issue in the discussion section. Both second and third order hydrodynamics are of contemporary interests as some recent works have called upon these theories in including mass effects and fluid-gravity duality. The predictions showed an increased importance of application of hydrodynamics to both massless and massive fluids as well as to compact systems [24–28].

Other recent works have directed hydrodynamics to the study of attractors which might indicate convergence of hydrodynamics coefficients. The works in Refs. [29,30] correspond to Anti-de Sitter-Conformal Field Theory (AdS-CFT), fluid gravity duality where hydrodynamics attractors up to order, $n = 240$ have been calculated. However the coefficients

^{*}younus.presi@gmail.com

[†]azwinndini.muronga@mandela.ac.za

show a convergence for $n \leq 5$, to which both second and third order theories are restricted. The works gave rise to the application of Borel resummation techniques to test the convergence. However the works are restricted to a massless limit of conformal theories and extending them to a massive particles regime could be carried out. Hydrodynamics could be studied at any temperature or particle density regimes as well as for both massive and massless regimes. Similar extensive works by Baier [31] with AdS-CFT and Jaiswal [32] with third order hydrodynamics in Boltzmann transport equation relaxation time approximation (BTE-RTA) have shown the calculation of attractors and convergence of hydrodynamics coefficients. Indeed it would be interesting to find the maximum order we can reach with hydrodynamics, before it is no longer valid.

In the current work we have extended the work done by Muronga to third order equations for the dissipative fluids [33] and presented it here as a test model for further development. The calculations are shown briefly in Sec. III. We have compared our calculations and results with earlier calculations by El *et al.* and Jaiswal. The results and discussions are reported in Sec. IV of the current paper, followed by conclusions.

II. EQUILIBRIUM AND NONEQUILIBRIUM DYNAMICS

In this section we discuss briefly the equilibrium and nonequilibrium dynamics. The dissipative fluxes which appear as time-dependant variables in the conservation equations, serve as major factors those push the fluid system out of equilibrium state. We also know from the laws of thermodynamics that entropy is conserved in ideal fluid. Because of the absence of dissipative forces, changes in the system are reversible. It is also known from earlier works that despite the nonphysical nature of perfect fluid, its dynamics are able to explain various phenomena in heavy ion collisions [34]. In real fluids, however, dissipative fluxes due to friction, stress, and heat flow cause the system to undergo irreversible processes and lead to an increase in entropy. At present, relativistic heavy ion collision experiments which are being conducted at LHC give us the context and opportunity to apply relativistic fluid dynamics and study the dissipative properties of quark gluon plasma (QGP) as well as hadron gases formed from QGP. Results from AdS-CFT have also suggested a small presence of viscous forces in QGP and give us a lower bound (Kovtun-Son-Starinets (KSS) bound) on $\frac{\eta}{s} = \frac{1}{4\pi}$ [35], where η is the shear viscosity and s is the entropy density of fluid system. Developing master equations and their solutions in order to simulate hydrodynamics evolution for relativistic fluids have been major challenges to researchers. Because of the presence of nonlinear terms, the formulation of equations becomes nontrivial even in the case of ideal hydrodynamics. Restrictions are also put on the equations by the laws of thermodynamics, and from the generalized expression from the equations one can derive the expression of the equation of state which could describe the thermodynamic states of the fluids. The theoretical formulation for the ideal/nondissipative hydrodynamics was given by Bjorken [36] which gave us the conservation equations for the energy-momentum tensor, number, and entropy densities. The Bjorken scaling solution has been applied to first, second,

and third order theories. The second order theories or M-IS theories use Grad's 14-moment method [37,38] and up to the second moment of the Boltzmann equation as approximation. M-IS included only linear terms in the dissipative equations and neglected nonlinear terms as well as terms such as derivatives of thermodynamic variables. The theories have limitations such as the reheating of the system, etc. Earlier discussions on IS theory in a simple one-dimensional Bjorken scaling expansion have also pointed out some unphysical results such as negative longitudinal pressure at small initial time. Thus higher order corrections along with the inclusion of nonlinear terms and derivatives of thermodynamic variables are studied to see if these effects can be reduced [33]. To include third order, both thermodynamic approach from Grad's 14-moment approximation by El *et al.* [39] and kinetic approach by Jaiswal [40,41] have been done. In both approaches by El and Jaiswal, respectively, a relativistic third order evolution equation for shear stress has been developed to study dissipative dynamics. The results could agree with exact solutions from Boltzmann transport equations. The approach to develop third order theory by Muronga takes the expansion of Grad's 14-moments up to quadratic terms, and gives a full expression for dissipative fluxes and thus entropy four-current up to third order. We will briefly discuss the formalism in the following section. As mentioned in the early seminal works of [29,30,42], gradient expansion techniques bring in a number of nonlinear terms and nonhydrodynamic modes. As to date these modes are yet to be fully understood, but they are important as they make equations of motion causal. As demonstrated in the above references, particularly through Maxwell-Cattaneo (MC) equations, the presence of nonhydrodynamic modes lead to finite signal propagation speed in contrast to first order or Navier-Stokes (NS) theories. In fact MC theory has derivatives in both space and time. This makes the resulting MC equations of motion hyperbolic, whereas the NS equations are parabolic in nature. Some of the consequences of nonlinear modes particularly on relaxation time has been discussed in the later sections.

III. FORMALISM

The basic formulation of relativistic hydrodynamics can be found in the literatures mentioned in previous sections. Here, a simple fluid with massless particles and no electromagnetic fields has been considered. The fluid is characterized by

$$N^\mu(x), \quad \text{particle four-current}, \quad (1)$$

$$T^{\mu\nu}(x), \quad \text{energy-momentum tensor}, \quad (2)$$

$$S^\mu(x), \quad \text{entropy four-current}. \quad (3)$$

The equations for the conservation of net charge and energy-momentum are given by

$$\partial_\mu N^\mu = 0, \quad (4)$$

$$\partial_\mu T^{\mu\nu} = 0. \quad (5)$$

Also, the second law of thermodynamics dictates

$$\partial_\mu S^\mu \geq 0. \quad (6)$$

The energy flow vector is similarly defined as

$$W^\mu = u_\nu T^{\nu\lambda} \Delta_\lambda^\mu = q^\mu + h v^\mu, \quad (7)$$

where $h = \frac{\varepsilon + P}{n}$ is the enthalpy, v^μ is the particle flow vector, and q^μ is the heat flow or heat four-current. In Eckart frame, the particle flux $v^\mu = 0$ which implies $W^\mu = q^\mu$. In the Landau and Lifshitz frame or energy frame, we have $W^\mu = 0$ which implies $q^\mu = -h v^\mu$.

The net charge four-current might be written of the form

$$N^\mu = n u^\mu + v^\mu. \quad (8)$$

In the Eckart frame, where there is no particle flux, the particle number density in the fluid rest frame is given by $n = \sqrt{N^\mu N_\mu}$. It can be shown that $u^\mu = \frac{N^\mu}{\sqrt{N^\mu N_\mu}}$ is the fluid four-velocity such that $u^\mu u_\mu = 1$, while the energy momentum tensor can be written as

$$T^{\mu\nu} = \varepsilon u^\mu u^\nu - (P + \Pi) \Delta^{\mu\nu} + 2q^{(\mu} u^{\nu)} + \pi^{(\mu\nu)}, \quad (9)$$

where $\varepsilon = u_\mu u_\nu T^{\mu\nu}$ is the energy density, P is the pressure in fluid rest frame, Π is the bulk viscous pressure, and $\pi^{(\mu\nu)}$ is shear stress tensor. $\Delta^{\mu\nu} = g^{\mu\nu} - u^\mu u^\nu$ is the projection tensor in three-dimensional space.

In the present calculation, Grad's 14-moments approximation has been used to develop the equations for dissipative fluxes. A system of relativistic fluid has been considered that departs slightly from the local thermal distribution. The distribution for particles in that system can then be written as

$$f(x, p) = f^{eq}(x, p) [1 + \Delta^{eq} \phi(x, p)], \quad (10)$$

where

$$f^{eq}(x, p) = A_0 \frac{1}{e^{\beta_\nu p^\nu - \alpha} - a} \quad (11)$$

is the equilibrium distribution function. The factor, Δ^{eq} , is expressed as $1 + a A_0^{-1} f(x, p)$ and $\phi(x, p)$ is the deviation/departure function. The definition of $f(x, p)$ has been used in Eq. (10) for the following expressions for number, energy-momentum tensor, and fluxes equations:

$$\begin{aligned} N^\mu(x) &= \int f(x, p) p^\mu dw, \\ T^{\mu\nu}(x) &= \int f(x, p) p^\mu p^\nu dw, \\ F^{\mu\nu\lambda}(x) &= \int f(x, p) p^\mu p^\nu p^\lambda dw, \end{aligned} \quad (12)$$

and it can be shown that particle four-current, energy momentum tensor, etc., are divided into equilibrium and nonequilibrium parts as follows:

$$\begin{aligned} N^\mu(x) &= N_{eq}^\mu(x) + \delta N^\mu(x), \\ T^{\mu\nu}(x) &= T_{eq}^{\mu\nu}(x) + \delta T^{\mu\nu}(x), \end{aligned} \quad (13)$$

where δN^μ , etc., is the nonequilibrium/deviation part from the corresponding quantity. The entropy four-current can also be divided into an equilibrium part and a nonequilibrium part as follows:

$$S^\mu(x) = S_{eq}^\mu(x) + \delta S^\mu(x). \quad (14)$$

Now to calculate δS^μ , we may similarly resort to Grad's 14-moment approximation with $S^\mu(x)$ defined as

$$S^\mu(x) = - \int dw p^\mu \psi(f), \quad (15)$$

where

$$\psi(f) = f(x, p) \ln [A_0^{-1} f(x, p)] - a^{-1} A_0 \times \ln \Delta(x, p). \quad (16)$$

Now we can expand $\psi(f)$ around $\psi(f^{eq})$ up to third order in derivative to obtain

$$\begin{aligned} \psi(f) &= -a^{-1} A_0 \ln \Delta^{eq}(x, p) \\ &+ [\alpha(x) - \beta_\nu(x) p^\nu] [f(x, p) - f^{eq}(x, p)] \\ &+ \frac{1}{2} [f^{eq}(x, p) A_0^{-1} \Delta^{eq}(x, p)]^{-1} [f(x, p) - f^{eq}(x, p)]^2 \\ &+ \frac{1}{6} [-f^{eq}(x, p) A_0^{-1} \Delta^{eq}(x, p)]^{-2} \\ &\times [f(x, p) - f^{eq}(x, p)]^3. \end{aligned} \quad (17)$$

Inserting the above equation in the entropy flux expression, i.e., Eq. (15) we have

$$\begin{aligned} S^\mu &= S_{eq}^\mu + \int dw p^\mu [\alpha(x) + \beta_\nu(x) p^\nu] (f - f_{eq}) \\ &- \frac{1}{2} \int dw p^\mu [f^{eq}(x, p) A_0^{-1} \Delta^{eq}(x, p)]^{-1} (f - f^{eq})^2 \\ &- \frac{1}{6} \int dw p^\mu [f^{eq}(x, p) A_0^{-1} \Delta^{eq}(x, p)]^{-2} (f - f^{eq})^3, \end{aligned} \quad (18)$$

where second, third, and fourth integration should give us first, second, and third terms of the entropy current, respectively.

A small linear departure function (non-equilibrium) $\phi(x, p)$ in $f(x, p)$ has been taken as

$$\begin{aligned} \phi(x, p) &= y(x, p) - y_{eq}(x, p) \\ &\approx \varepsilon(x) - \varepsilon_\mu(x) p^\mu + \varepsilon_{\mu\nu}(x) p^\mu p^\nu, \end{aligned} \quad (19)$$

where

$$y(x, p) = \ln [A_0^{-1} f(x, p) / \Delta(x, p)] \quad (20)$$

differs from its local equilibrium value, y_{eq} by quantity $\phi(x, p)$. The moments ε , ε_μ , and $\varepsilon_{\mu\nu}$ are assumed small. The expressions for these coefficients are given in the Appendix A of this paper.

After integration, the entropy four-current can be written up to third order or cubic in dissipative fluxes as

$$\begin{aligned} S^\mu &= S_1^0 u^\mu + S_1^1 \Pi u^\mu + S_2^1 q^\mu \\ &+ (S_1^2 \Pi^2 - S_2^2 q^\alpha q_\alpha - S_3^2 \pi^{2(\alpha\alpha)}) \beta u^\mu \\ &+ \beta (S_4^2 \Pi q^\mu + S_5^2 \pi^{(\mu\alpha)} q_\alpha) \\ &+ (S_1^3 \Pi^3 - S_2^3 \Pi q_\alpha q^\alpha + S_3^3 \Pi \pi^{2(\alpha\alpha)}) \\ &+ S_4^3 q_\alpha q_\beta \pi^{(\alpha\beta)} - S_5^3 \pi^{3(\alpha\alpha)} \beta u^\mu \\ &+ (S_6^3 \Pi^2 - S_7^3 q_\alpha q^\alpha + S_8^3 \pi^{2(\alpha\alpha)}) \beta q^\mu \\ &+ \beta (S_9^3 \Pi \pi^{(\mu\alpha)} q_\alpha + S_{10}^3 \pi^{2(\mu\alpha)} q_\alpha), \end{aligned} \quad (21)$$

where the coefficients S_n^m are calculated as functions of ε and n and are shown in Appendix A. The superscript in the coefficients denotes the order and the subscript labels the coefficient number in that order. The terms $\pi^{2(\alpha\alpha)} = \pi^{(\alpha\beta)}\pi_{(\alpha\beta)}$, $\pi^{3(\alpha\alpha)} = \pi^{(\alpha\beta)}\pi_{(\alpha\delta)}\pi_{\beta}^{\delta}$, etc., are written in shortened form. In case of second order theory, S_n^2 s are equivalent to the coefficients α_i and β_i shown in Ref. [17]. For thermodynamic processes, the entropy principle suggests $\partial_\mu S^\mu \geq 0$. The dissipative fluxes can be obtained either from the equations of the balance of the fluxes or from entropy principle. We may recall that at zeroth order the dissipative fluxes take their equilibrium values, $\Pi = \Pi_{eq} = 0$, $q^\alpha = q_{eq}^\alpha = 0$, and $\pi^{(\alpha\beta)} = \pi_{eq}^{(\alpha\beta)} = 0$. The complete third order equations of motion or relaxation equations of dissipative fluxes have been given in Appendices A and B.

A. Bjorken scaling solution

In the Bjorken scaling solution, the thermodynamic variables such as temperature, chemical potential, pressure, and dissipative fluxes are functions of proper time τ only. This means that the explicit transverse space derivatives of temperature, fluid velocity, coupling coefficients, etc., are absent. Also under such condition heat flow is shown to be $q^\mu = 0$ [15,18]. However this does not imply that the number density $n = 0$. In the current scenario $\varepsilon + P$ is the effective enthalpy, $P + \Pi + \pi$ is the longitudinal pressure, and $P + \Pi - \pi/2$ is the transverse pressure of the system. The four-velocity in Bjorken (1 + 1) dimensional expansion is defined as $u^\mu = (t/\tau, 0, 0, z/\tau)$, and the derivatives of the four-velocity are shown to be $\partial_\mu u^\mu = \frac{1}{\tau}$ and $u^\mu \partial_\mu = \frac{\partial}{\partial \tau}$. In the comoving frame, the shear tensor is diagonal with a positive shear pressure: $\pi_{\mu\nu} = \text{diag}(0, \pi/2, \pi/2, -\pi)$. The parentheses on the indices denote symmetrization and skew-symmetrization as follows:

$$\begin{aligned} a^{(\mu\nu)} &\equiv \frac{1}{2}(a^{\mu\nu} + a^{\nu\mu}), \\ a^{(\mu\nu)} &\equiv (\Delta_\alpha^{(\mu} \Delta_\beta^{\nu)} - \frac{1}{3} \Delta^{\mu\nu} \Delta_{\alpha\beta}) a^{\alpha\beta}. \end{aligned} \quad (22)$$

Thus in Bjorken (1 + 1) dimensional scaling, the first order transport equation could be reduced to

$$\Pi = -\zeta \frac{1}{\tau}, \quad (23)$$

$$q^\mu = 0, \quad (24)$$

$$\pi = \frac{4}{3} \eta \frac{1}{\tau}. \quad (25)$$

From the entropy principle, the general equation in dissipative fluxes can be shown to be

$$\begin{aligned} T \partial_\mu S^\mu &= \frac{\Pi^2}{\zeta} - \frac{q_\mu q^\mu}{\kappa T} + \frac{\pi_{\mu\nu} \pi^{\mu\nu}}{2\eta} \geq 0 \quad \text{with} \\ &\zeta, \kappa, \eta \geq 0, \end{aligned} \quad (26)$$

where ζ , κ , and η are bulk viscous, thermal conductivity, and shear viscous coefficients, respectively.

The expressions for shear $\pi^{\mu\nu}$, bulk pressures Π , and heat q^μ flux derived from Eqs. (21) and (26) have been shown in Appendix B. In the present calculations where we are working

in Bjorken scaling solution, and the ultrarelativistic regime (massless fluid particles), only the shear pressure equation remains to be solved. The third order shear pressure expression thus obtained as

$$\begin{aligned} \pi^{(\mu\nu)} &= -2\eta T \Delta^{\alpha\mu} \Delta^{\beta\nu} \left[-\partial_{(\alpha} u_{\beta)} + 2\beta S_3^2 (u_\lambda \partial^\lambda \pi_{(\alpha\beta)}) \right. \\ &\quad + \pi_{(\alpha\beta)} \partial^\lambda (\beta u_\lambda S_3^2) + 3\beta S_3^3 (u_\lambda \partial^\lambda \pi_{(\alpha\delta)} \pi_{\beta}^{\delta}) \\ &\quad \left. + \pi_{(\alpha\delta} \pi_{\beta)}^{\delta} \partial^\lambda (\beta S_3^3 u_\lambda) \right]. \end{aligned} \quad (27)$$

Using Eq. (27), the third order equation can also be written as

$$\begin{aligned} u_\lambda \partial^\lambda \pi^{(\mu\nu)} &= -\frac{\pi^{(\mu\nu)}}{\tau_\pi} + \frac{2\eta \partial^\mu u^\nu}{\tau_\pi} - \frac{2\eta T}{\tau_\pi} \pi^{(\mu\nu)} \partial^\lambda \left(\frac{S_3^2}{2T} u_\lambda \right) \\ &\quad - \frac{3\eta S_3^3}{\tau_\pi} (u_\lambda \partial^\lambda \pi^{(\mu\delta)} \pi_{\delta}^{\nu)}) \\ &\quad - \frac{2\eta T}{\tau_\pi} \pi^{(\mu\delta} \pi_{\delta}^{\nu)} \partial^\lambda \left(\frac{S_3^3}{2T} u_\lambda \right), \end{aligned} \quad (28)$$

where $\tau_\pi = 2\eta S_3^2$ is relaxation time for the shear pressure. The coefficient S_3^2 is taken to be $\approx 9/4\varepsilon$ in the ultrarelativistic limits. We have used the equation of state (EoS) due to the assumed ultrarelativistic scenario to be $\varepsilon = 3P$.

After simplification and keeping all the terms, the final equations for shear pressure for third order viscous and massless fluids is found to be

$$\begin{aligned} \dot{\pi} &= -\frac{\pi}{\tau_\pi} - \frac{1}{2} \frac{\pi}{\tau} + \frac{3}{10} \frac{\varepsilon}{\tau} + \frac{5}{8} \frac{\pi}{\varepsilon} \dot{\varepsilon} - \frac{3}{2} \frac{\pi^2}{\varepsilon \tau} \\ &\quad + \frac{27}{8} \frac{\pi^2}{\varepsilon^2} \dot{\varepsilon} - \frac{12}{5} \frac{\pi}{\varepsilon} \dot{\pi}. \end{aligned} \quad (29)$$

Also in (1 + 1) dimensional Bjorken flow, the energy and number density equations calculated from Eqs. (8) and (9) are similarly given by

$$\dot{\varepsilon} = -\frac{\varepsilon + P}{\tau} + \frac{\pi}{\tau}, \quad \dot{n} = -\frac{n}{\tau}. \quad (30)$$

The shear differential equation shown in Eq. (28) has an order by order implication on the final output or calculated energy and entropy densities. The effects due to the inclusion of various orders on the solutions of dissipative equations will be discussed in the next section.

IV. RESULTS AND DISCUSSIONS

Pressure isotropy is the measure of a system's isotropization and indicates the system's return to its equilibrium state. It is calculated as the ratio of longitudinal pressure (P_L) to transverse pressure (P_T) of the system. A system of quarks and gluons in equilibrium behaves like a fireball where P_L equals P_T , and the ratio remains unity and independent of time. But with the presence of viscous forces, the ratio diverges from unity (i.e., the system is out of equilibrium) but gradually returns to equilibrium with time. Usually the collision axis for the heavy ions is taken to be a longitudinal axis (viz. z axis) with zero momentum along 'x' or 'y' (transverse) directions. After the collision, because of the presence of viscous drag along the z axis, the particles tend to push more on the transverse direction than the longitudinal direction.

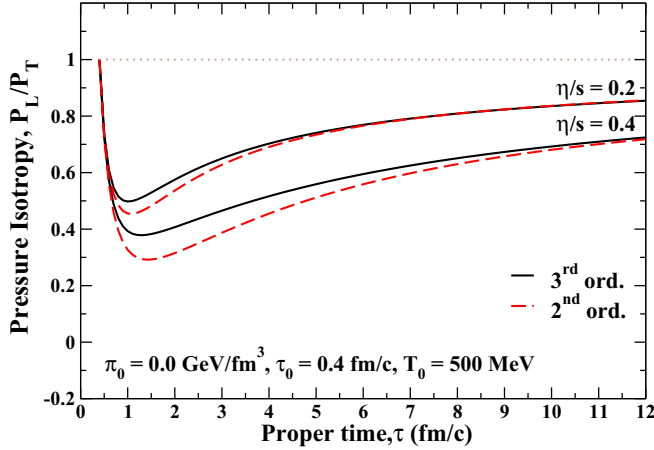


FIG. 1. Pressure isotropy of relativistic fluid using second and third order shear equations with $\pi_0 = 0$.

However the system due to particle interaction and decreasing dissipative fluxes, the pressure continues to build along the z axis and, if given enough time, the system could return to equal pressures along both longitudinal and transverse axes. Let us now move to a discussion of the results. We may recall that calculations have been done in the $(1+1)$ dimensional Bjorken scenario with boost-invariance assumed along the z axis.

Figure 1 shows pressure isotropy as a function of proper time for an expanding fluid with an initial condition matching that of an ideal relativistic fluid. The figure shows a comparison between shear pressure in second and third order equations. Two different values of η/s have been used. Because of the initial $\pi_0 = 0 \text{ GeV/fm}^3$ the fluid is initially isotropic and thereafter the dissipative fluxes put the system rapidly out of equilibrium. The system tries to get back to equilibration and the trends show a continuous rise in isotropization although a certain degree of saturation already sets after 4–5 fm/c. The ideal scenario is represented by a unit valued line (dotted). Initially the second order shows a greater dip than the third order, which indicates that third order tends to limit or decrease the dissipative effects brought in by lower orders. One may also find that higher values of η/s bring in more of a difference between second and third order shear equations. An initial temperature of $T_0 = 500 \text{ MeV}$ at QGP formation time of $\tau_0 = 0.4 \text{ fm/c}$ has been used in the calculations. It is interesting to mention that in some earlier studies higher orders beyond third order have been considered by El *et al.* and the seminal paper has heuristically explained that a higher order beyond third might increase the shear effects and observables might be closer to second order. However, it is also suggested in that literature that the effects might be oscillatory in nature if more ordered corrections are taken in the picture. This is yet to be studied more extensively [39].

Figure 2 shows pressure isotropy when initial shear pressure is changed from an ideal fluid to $\pi_0 = P_0$. We also recall that while deriving transport equations, we assumed that the dissipative fluxes should be small as compared to

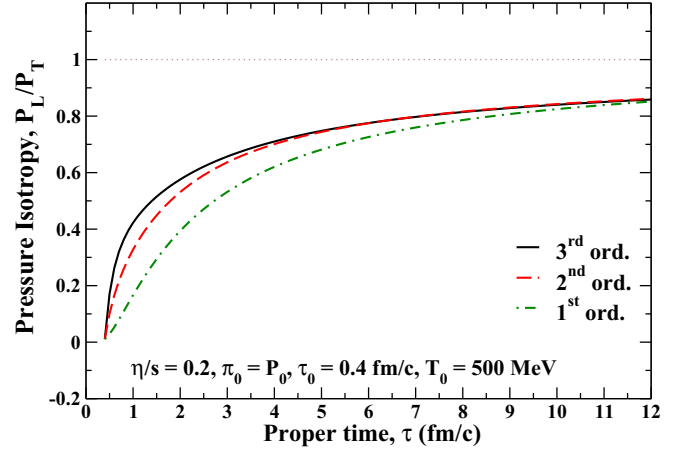


FIG. 2. Pressure isotropy of relativistic fluid using second and third order shear equations with $\pi_0 = P_0$.

the primary physical quantities (ε , n , P). In terms of π this condition can be written as $(\pi^{\mu\nu}\pi_{\mu\nu})^{1/2} < P$. In general the thermodynamic quantities will decrease with time as long as the condition $\pi \ll \varepsilon + P$, which in our case is $\pi_0 \ll 4P_0$. A moderate value of $\pi_0 \leq P_0$ has been used to avoid negative effective enthalpy and negative longitudinal pressure. Unlike the first order theories such limitations could be put on initial conditions in both second and third order theories. But for investigative studies one may relax this binding on π_0 to $4P_0$. The quantity P_L/P_T rises rapidly for the second and third order equations similar to the previous figure but the rates decrease and the curves try to merge beyond 6 fm/c. The first order result starts slower but tends to merge around 12 fm/c. Here too, the inclusion of third order decreases the effects of dissipative fluxes when compared to second order and first order shears. The initial temperature and time identical to Fig. 1, and a modest value of $\eta/s = 0.2$ have been used for this plot.

Next we move over to a comparison between various models which incorporated third order viscous hydrodynamics.

To begin with Figs. 3 and 4, it can be stated that values of the coefficients in relaxation equations from models differ from each other, respectively. The models used for comparison are referred here as El I. (AE), a third order thermodynamic theory, Jaiswal I. (AJ), a third order kinetic theory, and the current work, Muronga *et al.* (AM) which is based on third order theory based on thermodynamic entropy principle. The differential equations in these models have been found to be very sensitive to the values of coupling coefficients. One may also find that certain terms have been neglected in Muller-Israel-Stewart theories for second order because of their nonlinearity. The Muronga *et al.* model has included these terms in developing the shear differential equations. Figures 3 and 4 aim to highlight the sensitivity of values of the coefficients and terms used in the models. The model by AM calculates the full expansion of the entropy four-current using Grad's 14-moments theory. As approximations, mass of fluid particles and heat flux have been neglected in order to obtain a very simple picture of how viscous drag forces work within

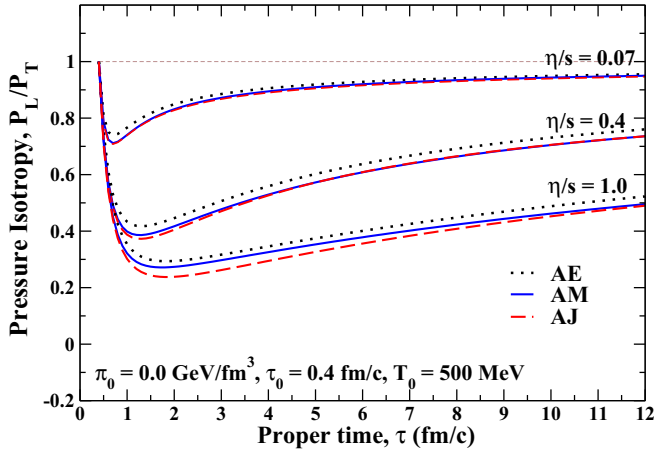


FIG. 3. Comparison of models on time evolution of pressure isotropization for different η/s values. Muronga *et al.* (AM) denotes inclusion of $\partial_i S_3^2$ and $\partial_i S_3^3$ terms in the third order equation.

the system. Also compared to the AE model, terms of order 4 in π/ε have also been included in the AM model. As seen from the figure, the models do not differ much for lower η/s values. For higher values of the parameter, the models differ by a small magnitude at low τ while for at later times they tend to merge. Figures 3 and 4 also differ from each other at the starting point of the curve due to the choice of initial values of π_0 . However the evolution of pressure isotropy ratios show a similar trend after $\tau = 2$ fm/c in both figures. The effects of various terms in Eq. (28) [simplified into Eq. (29)] will be discussed for Figs. 6 and 7.

In Fig. 5 the pressure isotropy ratio P_L/P_T calculated from current model (AM) has been compared to results from BAMPS transport theory. BAMPS data points have been extracted from El *et al.*'s paper which has up to $\tau = 4$ fm/c and hence the figure has a shorter x-axis range compared to other figures. The main focus of this plot is to highlight the difference between the transport calculation and effective third order theory shown in the current work. The BAMPS

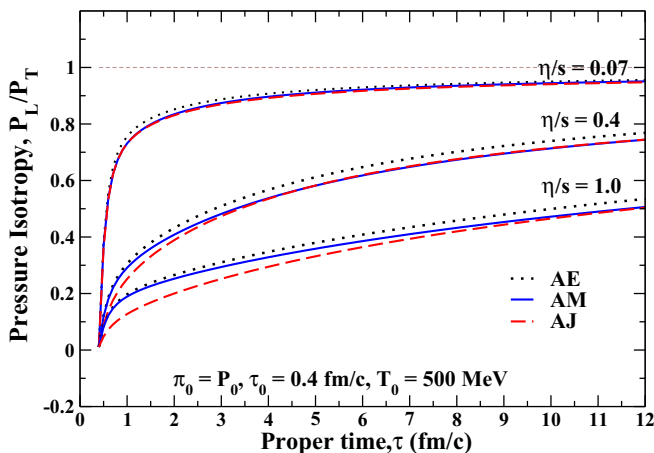


FIG. 4. Comparison of models on time evolution of pressure isotropization for different η/s values and for $\pi_0 = P_0$.

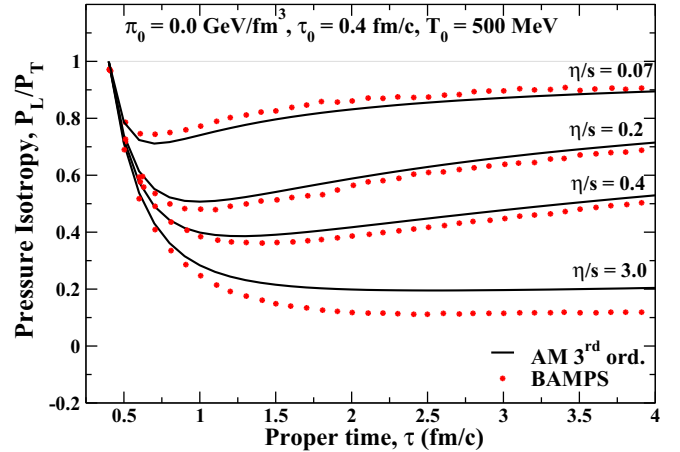


FIG. 5. Comparison pressure isotropy ration from AM third order theory with BAMPS transport calculation for different η/s .

exhibits larger transverse pressure compared to the AM model for η/s values ≥ 0.2 . The ratio however shows a similar trend for both models as the system evolves with time.

In Figs. 6 and 7, Eq. (28) has been dissected and discussed term by term. If Eq. (28) is simplified and the first two terms on the right-hand side (r.h.s.) of the equation are considered, they give us a Maxwell-Cattaneo (M-C) like equation. As known from earlier studies, the M-C equation has been used to study the propagation of second sound in the presence of dissipative heat flux in materials [43]. One may draw an analogy and write

$$\frac{dq}{dt} = -\frac{q}{t_0} + k \frac{\Theta}{t_0} \iff \frac{d\pi}{d\tau} = -\frac{\pi}{\tau_\pi} + \frac{2\eta}{\tau} \frac{1}{\tau_\pi}, \quad (31)$$

where t_0 is the relaxation time, Θ is absolute temperature. We have labeled the solutions to the above set of terms in the AM equation as M-C in the figures. In addition we have also compared the solutions of Muller-Israel-Stewart equations (M-IS) and second order theory. One may recall that certain terms such as $\Pi \partial_i \varepsilon$, $\pi_{(\alpha\beta)} \partial_i \varepsilon$, $q_\alpha \partial_i n$ and consequently $\partial_i S_3^2$ and $\partial_i S_3^3$ have been neglected in M-IS equations due to their non-linear nature [13]. MI-S theory developed for second order shows that these terms (including vorticity terms) may not be explicit from the entropy principle or kinetic theory [44]. However the extra terms are consistent with conformal theories [31,45].

It can be seen from the figures that the terms $\partial_i S_3^2$ and $\partial_i S_3^3$ have discernible effects on solutions. The calculations are done at a moderate $\eta/s = 0.4$. The differences in the solutions are more visible at low τ . The M-C equation gives more shear pressure and energy density (see Fig. 6) for low and intermediate time, and consequently the pressure isotropy parameter, P_L/P_T , calculated from the M-C equation, (see Fig. 7) goes below zero for $\tau < 3$ fm/c. MI-S equations which have second order shear terms do not contain a $\partial_i S_3^2$ term. As a result the solutions to the M-IS equation although closer to AM second order theory, have considerable differences with it and thus the effects of nonlinear terms could be highlighted. AM second order theory decreases the overall dissipative

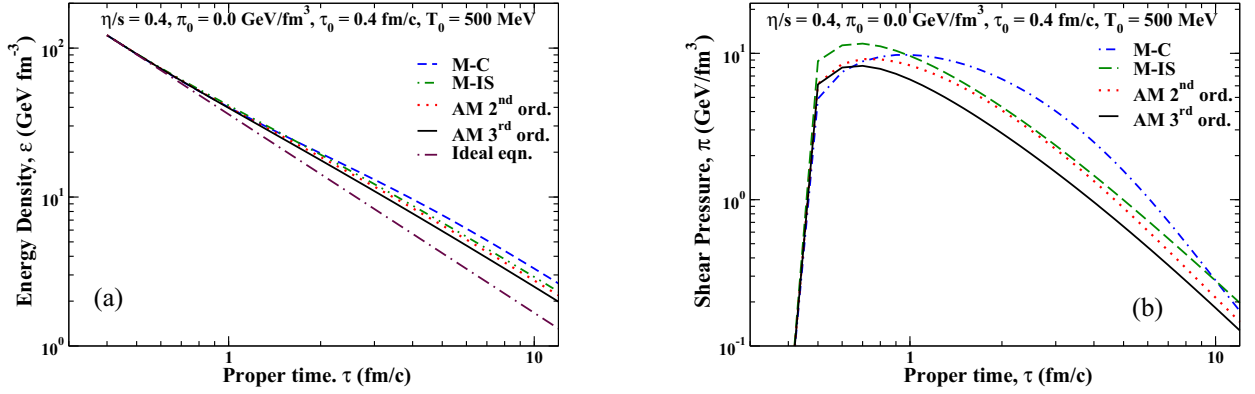


FIG. 6. (a) Energy density solution for Maxwell-Cattaneo–like equations, Muller-Israel-Stewart theory, and Muronga *et al.* second and third order equations. (b) Solutions for shear pressure for the models mentioned.

effects of the shear. AM third order theory shows a further decrease in shear pressure and almost merges with second order solution around $\tau = 12$ fm/c. Third order energy density solution also differs from an ideal solution by a magnitude. This difference however may be due to the assumed value of $\eta/s = 0.4$. The effects of the η/s on ordered theories have already been discussed in the context of Fig. 1.

In Eq. (28) the term $-\frac{3\eta S_3^3}{\tau_\pi} u_\lambda (\partial^\lambda \pi^{\mu\delta}) \pi_\delta^\nu$ appearing in the third order shear relaxation equation is nonlinear and has been simplified into the last term in Eq. (29). The ratio $\frac{3\eta S_3^3}{\tau_\pi} \pi \approx \frac{\pi}{\varepsilon}$ has been neglected in Ref. [39] for all time. However for earlier times when $\tau < \tau_\pi$, this term proves to be relevant. This is evident in Fig. 8, where for a moderate value of $\frac{\eta}{s} = 0.4$, the calculation of the ratio $\frac{\pi}{\varepsilon}$ has approximate values between 0.161 and 0.11 at $\tau = 1.0$ fm/c to 7 fm/c but drops down to 0.060 around $\tau = 12$ fm/c. Hence for the major part of QGP evolution this term although nonlinear becomes a contributing factor.

Following the above discussion, the term $3\eta S_3^3 \pi$ can be referred to as a relaxation time that comes from the third order equation. This term also provides a correction factor to second

order relaxation time τ_π in Eq. (28) as follows:

$$\begin{aligned} \tau_\pi \left(g^{\mu\delta} + \frac{3\eta S_3^3}{\tau_\pi} \pi^{\langle\mu\delta\rangle} \right) u_\lambda \partial^\lambda \pi_\delta^\nu & \\ = -\pi^{\langle\mu\nu\rangle} + 2\eta \partial^\mu u^\nu - 2\eta T \pi^{\langle\mu\nu\rangle} \partial^\lambda \left(\frac{S_3^2}{2T} u_\lambda \right) & \\ - 2\eta T \pi^{\langle\mu\delta\rangle} \pi_\delta^\nu \partial^\lambda \left(\frac{S_3^3}{2T} u_\lambda \right), \quad \text{or} & \\ \tau_\pi^{\langle\mu\delta\rangle} u_\lambda \partial^\lambda \pi_\delta^\nu & \\ = -\pi^{\langle\mu\nu\rangle} + 2\eta \partial^\mu u^\nu - 2\eta T \pi^{\langle\mu\nu\rangle} \partial^\lambda \left(\frac{S_3^2}{2T} u_\lambda \right) & \\ - 2\eta T \pi^{\langle\mu\delta\rangle} \pi_\delta^\nu \partial^\lambda \left(\frac{S_3^3}{2T} u_\lambda \right), & \end{aligned} \quad (32)$$

where $\tau_\pi^{\mu\delta} = \tau_\pi (g^{\mu\delta} + \frac{3\eta S_3^3}{\tau_\pi} \pi^{\mu\delta})$ can be termed as the modified relaxation time for the third order shear viscous pressure. $\tau_\pi^{\mu\delta}$ is in a tensorial form and depends on the form of the shear pressure tensor. We find that third order correction explicitly

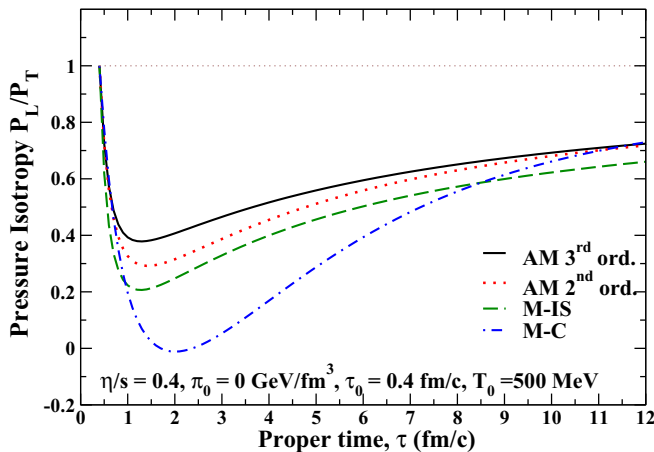


FIG. 7. Time evolution of pressure isotropy for various terms in shear pressure differential equation.

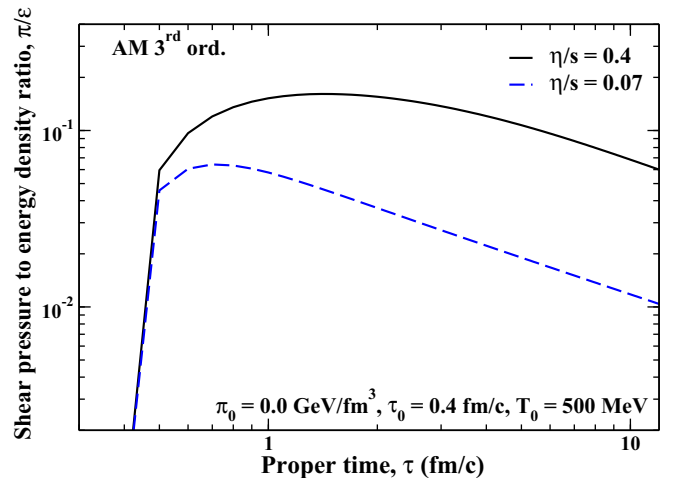


FIG. 8. Time evolution of shear pressure to energy density ratio for various $\frac{\eta}{s}$ values at $T_0 = 500$ MeV and $\tau_0 = 0.4$ fm/c.

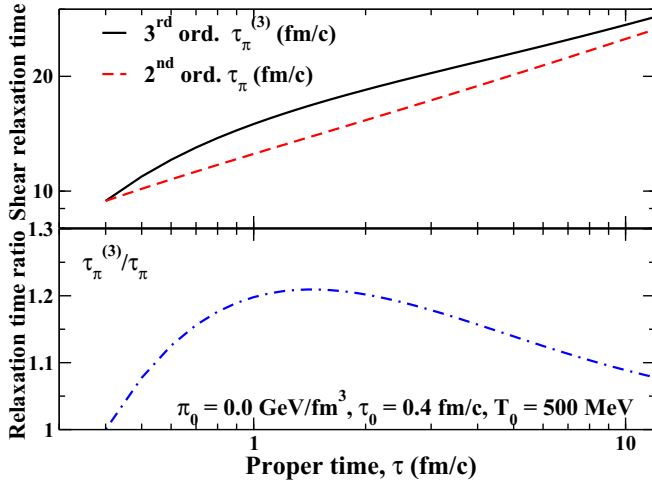


FIG. 9. Time evolution of shear relaxation time for $\eta/s = 0.4$ values at $T_0 = 500$ MeV and $\tau_0 = 0.4$ fm/c.

brings in the shear fluxes in the expression for the relaxation time. This was absent in second order. Another interesting feature is that no direction dependent effects were present in second order relaxation time whereas in third order theory we have τ_{π}^{xx} , τ_{π}^{yy} , and τ_{π}^{zz} along x , y , and z directions. In the case of the Bjorken (1 + 1) dimensional scenario, the effect of the correction term for relaxation time has been obtained from Eq. (29) and the modified relaxation time, $\tau_{\pi}^{zz} = \tau_{\pi}^{(3)}$ is shown in Fig. 9. The figure shows a clear difference between second and third order effects. Thus it would be interesting to study the effects of various ordered theories on the relaxation times.

Let us now discuss the effects of shear viscosity to entropy ratio on the pressure isotropization. It can be shown from transport models that parameter η/s shows a coupling between medium particles or the strength of particles' interaction. The parameter could be shown to be $\eta/s \approx 0.066 * [\alpha_s^2 \ln(\alpha_s^{-1})]^{-1}$ ($N_f = 3$ and $0 \ll \alpha_s \ll 1$) [46,47]. The equation shows the viscosity to entropy ratio as a function of strong coupling. In the current calculation, η/s has been treated as a parameter with constant values which also indicate constant values for strong coupling assumed in our calculations. However it should be recalled that strong coupling is a running coupling and depends on the system temperature or momentum transfer during particle interaction.

Figure 10 shows the dependence of the shear viscosity to entropy ratio on pressure isotropization. As η/s is increased, the system is removed further from equilibrium and at high values of $\eta/s = 1.0-3.0$ (highly viscous fluid), the ratio P_L/P_T is almost flat after 2 fm/c with a slow rise. This indicates that fluid with high viscosity may not return to isotropy quickly. The earlier studies [18] have however shown that second order theories break down beyond $\eta/s \approx 0.4-0.5$, possibly limiting the maximum values for η/s .

For a very low value of $\eta/s = 0.07$, the pressure isotropy ratio goes closer to unity around the time $\tau = 10-12$ fm/c. This suggests the importance for the study of time or length scale dependence of isotropization or equilibration of viscous fluids.

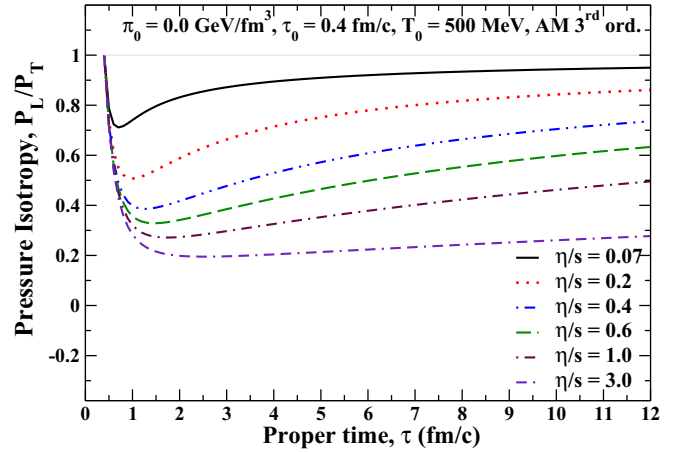


FIG. 10. Time evolution of pressure isotropy for various η/s values at $T_0 = 500$ MeV and $\tau_0 = 0.4$ fm/c.

Figure 11 shows proper-time evolution of shear pressure with two different initial shear pressure. $\pi_0 = 0$ matches that of ideal fluid, while $\pi_0 = P_0$ provides a high initial dissipative flux. The results from second and third order equations for an ideal fluid-like initial condition, rise rapidly from zero but tend to fall off more quickly when compared to the corresponding results using a large initial shear. Irrespective of the initial conditions both second and third order theories bring down the dissipative fluxes as compared to the first order theory. Also third order theory brings shear viscosity to lower value than the second order although the difference decreases as the system evolves in time. Overall the decrease of shear pressure with time indicates that the system attempts to return to local equilibration (perfect fluid).

In Fig. 12, the proper-time evolution of QGP's energy density calculated from ideal, first, second, and third order equations has been shown. The top plot shows time evolution of energy density for a moderate value of $\eta/s = 0.4$, and two initial values of $\pi_0 = 0$ and P_0 . The results are shown for an initial temperature of $T_0 = 500$ MeV and $\tau_0 = 0.4$ fm/c.

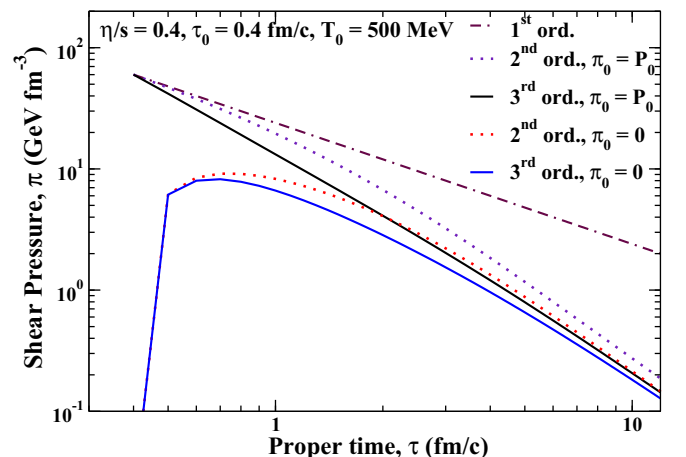


FIG. 11. Comparison of different orders of shear pressure for two initial conditions of $\pi_0 = 0.0$ and $\pi_0 = P_0$.

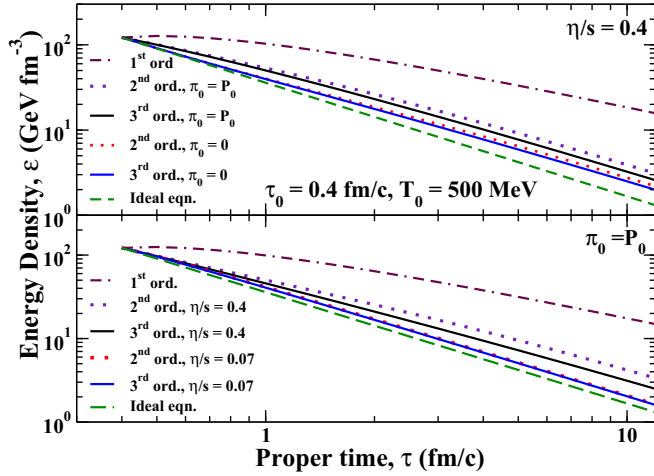


FIG. 12. Comparison of energy density calculated from second and third order theories with ideal and first order equation. (Top) Two different initial shear values of $\pi_0 = 0.0$ and $\pi_0 = P_0$ are used at fixed $\eta/s = 0.4$. (Bottom) Two different η/s values of 0.07 and 0.4 at fixed π_0 have been used.

The bottom plot keeps $\pi_0 = P_0$ fixed while varying η/s . The ideal equation in the Bjorken (1 + 1) dimensional expansion shows the expected trend with energy density decreasing as $\approx \frac{1}{\tau^{4/3}}$. The first order equation shows a slight rise in the energy content of the system to a peak until 1 fm/c and then decreases slowly. The peak is more visible in the top plot for the fixed value of η/s . The first order theory differs from the ideal scenario by an order of magnitude around 12 fm/c in both plots. The second and third order brings down this difference to values closer to the ideal situation. We may also notice from both plots that initial value of $\pi_0 = 0.0 \text{ GeV}/\text{fm}^3$ or $\eta/s = 0.07$ brings energy density closer to the ideal case than $\pi_0 = P_0$ or $\eta/s = 0.4$.

Similar to Fig. 12, time evolution of temperature of the relativistic fluid is shown in Fig. 13. In both plots ideal flow quickly takes an initial temperature of 500 MeV to an assumed critical temperature of $T_c \simeq 155\text{--}160 \text{ MeV}$ [48,49] (when hadronization sets in) around $\tau = 10\text{--}12 \text{ fm}/c$ approximately. The first order theory is still far above T_c by a factor. The ideal and first order theories thus represent two opposite and extreme scenarios of dissipative fluids. In general for the ideal and first order equations, the temperature varies as

$$\frac{T}{T_0} = \left[\frac{\tau_0}{\tau} \right]^{1/3} \left\{ 1 + \frac{R_0^{-1}}{2} \left(1 - \left[\frac{\tau_0}{\tau} \right]^{2/3} \right) \right\}, \quad (33)$$

where T_0 and R_0 are temperature and Reynolds number at $\tau = \tau_0$. The Reynolds number is given by $\frac{\varepsilon + P}{\pi}$. With $R_0^{-1} = 0$, the temperature evolves in the ideal condition (perfect fluid). For ideal fluid, we get $T \simeq 160 \text{ MeV}$ at $\tau = 12 \text{ fm}/c$. Also for $\tau = \tau_0$, the temperature for the two extreme scenarios start from the same point while higher order theories lie in between. The third order equations could bring the temperature closest to the ideal scenario for initial conditions such as $\pi_0 = 0$, $\eta/s = 0.4$ and $\pi_0 = P_0$, $\eta/s = 0.07$. One may infer that choice of initial

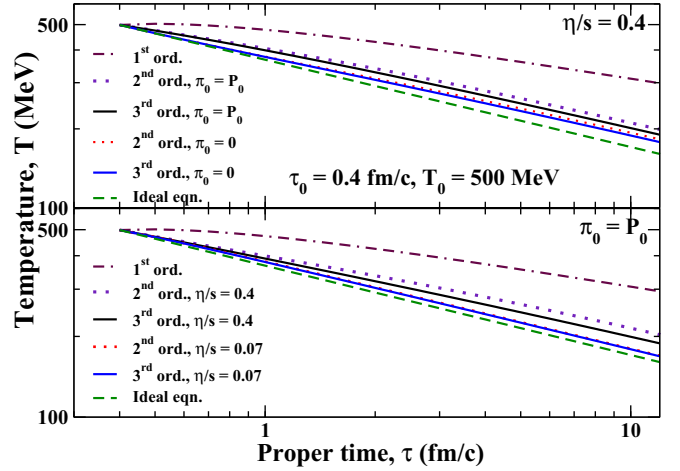


FIG. 13. Comparison of temperature evolution between various orders of dissipative equations at initial LHC temperature of 500 MeV. Two different initial shear values of $\pi_0 = 0.0$ and $\pi_0 = P_0$ are used.

conditions has considerable effects on temperature evolution. Detailed study of transport coefficients used as initial conditions could be carried out using various transport calculations viz. ultra-relativistic quantum molecular dynamics (UrQMD), Boltzmann approach for many parton scattering (BAMPS), parton cascade model/Bass-Muller-Srivastava (PCM-VNI/BMS), etc. Next we move onto a discussion of entropy density.

The entropy density, s has a direct relation to the particle production. The enhancement of the production of particles generates more entropy. However, with expansion of the medium or system, as temperature falls off, particle production decreases along with it. Figure 14 shows a change in the entropy density with time. Ideal evolution gives a rapid entropy decrease as the system nears the critical temperature, assumed to be around 155–160 MeV. The first order theories on the other hand decrease most slowly and differ from the

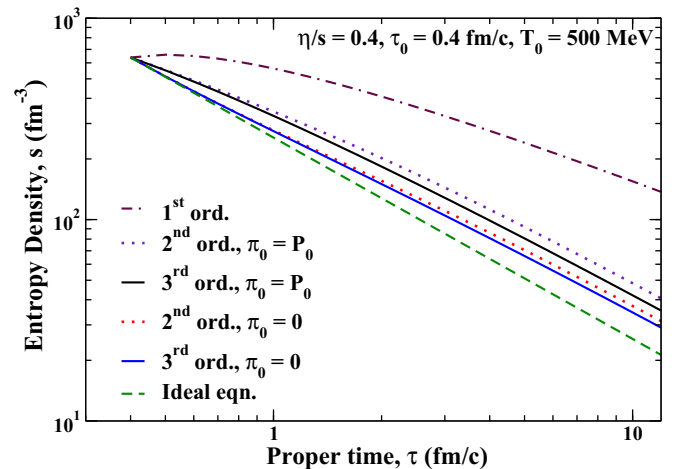


FIG. 14. Proper-time evolution of entropy density for various orders of shear pressure equation.

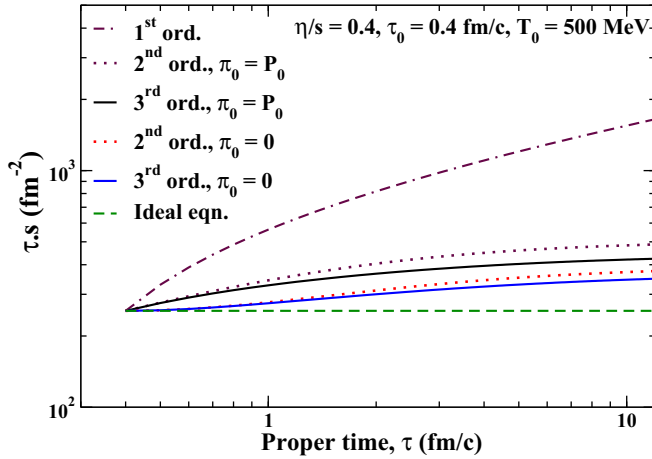


FIG. 15. Time evolution of τs with proper time and comparison between orders for $\pi_0 = 0.0$ and $\pi_0 = P_0$.

ideal scenario by an order of magnitude. The third order theory on the other hand brings the system closer to the ideal scenario although it differs by a small factor.

It is known from Bjorken (1 + 1)D hydrodynamics that in the ideal scenario, τs should be conserved over time where τ is the proper time and s is the entropy density. The ideal scenario in Fig. 15 shows the conservation of the quantity as expected from Bjorken's hydrodynamics. The first order theory on the other hand keeps generating more and more entropy which makes the trend rise although there is a small sign of saturation at a later time. The higher orders, particularly third order, bring this increasing trend down although there is a small increase in the value. However the saturation for the third order develops earlier than the first and second order theories. One may notice that zero initial shear pressure puts the curves closer to the ideal situation. The calculation is done for a moderate value of $\eta/s = 0.4$ at an initial temperature of $T_0 = 500$ MeV and $\tau_0 = 0.4$ fm/c. It can be shown from Bjorken hydrodynamics [36,50,51] that in case of ideal fluid

$$\tau_0 s_0 = \tau s = \frac{2\pi^4}{4\pi\zeta(3)\pi R_T^2} \frac{dN}{dy}, \quad (34)$$

where $\frac{dN}{dy}$ is the observed particle rapidity density distribution and R_T is the transverse radius of the system. We have assumed chemical freeze-out time to be equal to hadronization or critical time and ignored hadronic medium effects. Although an exact analytical expression for second and third orders is not possible but using Eq. (33) and the expression $s = 4a T^3$ one can have a straightforward expression for ideal and first order

$$\tau s = \tau_0 s_0 \left[1 + \left\{ \frac{R_0^{-3}}{8} \left(1 - \frac{\tau_0^{2/3}}{\tau^{2/3}} \right)^3 + \frac{3R_0^{-1}}{2} \right. \right. \\ \left. \left. \times \left(1 - \frac{\tau_0^{2/3}}{\tau^{2/3}} \right) + \frac{3R_0^{-2}}{4} \left(1 - \frac{\tau_0^{2/3}}{\tau^{2/3}} \right)^2 \right\} \right], \quad (35)$$

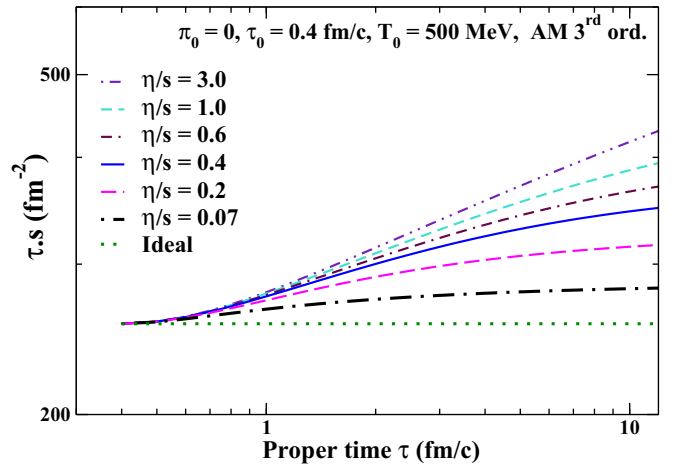


FIG. 16. Time evolution of τs with proper time and comparison between values of η/s for $\pi_0 = 0.0$, $\tau_0 = 0.4$ fm/c, and $T_0 = 500$ MeV.

where the terms in $\{\dots\}$ can be termed as the first order correction factor to the ideal equation. Hence we can write to the first approximation that

$$\tau s = \tau_0 s_0 [1 + F_1(\tau)], \quad (36)$$

where $F_1(\tau)$ is the first order correction factor and might be calculated analytically for higher orders. This also shows that correction to multiplicity density can be approximately treated as an additive quantity to the ideal scenario. In our case the calculations have been done for the midrapidity where boost-invariance along longitudinal direction is assumed. From the above relation and results from Fig. 15 at $\tau = 12$ fm/c, one finds for the ideal scenario $\frac{dN_{ch}}{d\eta} = 1749$ which is 14% lower than experimental data ≈ 2035 at LHC energy of $\sqrt{s_{NN}} = 5.02$ TeV [52]. Similarly, for the initial conditions of $\pi_0 = 0$ and $\eta/s = 0.4$, the third order equation gives $\frac{dN_{ch}}{d\eta} = 2390$ which is about 17% more than data and 36% more than the ideal case. Second order equation gives $\frac{dN_{ch}}{d\eta} = 2578$ which is 26% more than the experimental value and 47% more than the ideal scenario. The first order theory on the other hand gives $\frac{dN_{ch}}{d\eta} = 11741$ which is 7 times higher than the ideal value or 500% increase approximately.

As mentioned earlier, initial conditions for transport coefficients play a vital role in the precise calculation of entropy or particle production. This is shown in Fig. 16 for third order theory. Keeping $\pi_0 = 0$, if η/s is taken to be 0.07, $\frac{dN_{ch}}{d\eta}$ at $\tau = 12$ fm/c is calculated to be 1927 which is 10% more than ideal equation but 5% less than the experimental value. Similarly if we have $\eta/s = 0.2$, we have $\frac{dN_{ch}}{d\eta} = 2157$ which is 23% more than ideal equation and 6% more than experimental results. Similar calculation with $\eta/s = 0.07$ and 0.2 in second order theory (not shown in figure) gives $\frac{dN_{ch}}{d\eta} = 1931$ and 2222 which are 5% less and 10% more than the experimental values, respectively. If one uses first order theory to calculate $dN_{ch}/d\eta$, it is found to be 3936 for $\eta/s = 0.07$ at $\tau = 12$ fm/c. It can be seen that first order gives particle production 93% more than experimental data. Following the

above results, one could put limits on the values of η/s through a calculation of particle multiplicity density. However different order theories give a slightly different range for the parameter although part of this range overlaps. On the other hand, such dissimilarities might also limit the universal adaptation of a particular ordered theory for dissipative fluids. This aspect would be further investigated and reported.

It could be recalled that no effects due to dissipative heat flow as well as from bulk viscous pressure have been included in the present calculations. Bjorken scaling solution excludes the heat flow coefficient and the ultrarelativistic scenario neglects effects of bulk viscosity. Consequently most of the terms in Eq. (21) are absent and give us a very simplistic picture. The goal of developing the third order viscous hydro-equations is to highlight the coupling coefficients S_n^m s which display not only the correlation of dissipative fluxes among themselves but also with each other. Such correlations are absent in second order theories. In our current work the Bjorken scenario has eliminated the possibilities of correlations among fluxes except the shear viscous pressure term, $\pi_{\alpha\beta}\pi^{\alpha\beta}$. The inclusions of the other two important fluxes and all types of correlations should bring in changes in the production of entropy [see Eq. (26)], energy density, relaxation time, and other rich components and these effects must be extensively studied in the near future. No hadronic medium effects have been included in our simple model. It naively assumes the chemical freeze-out scenario occurs at the critical temperature itself. Relaxing this condition should bring in an extra particle production from the hadronic medium mainly from hadron decay channels. Earlier studies on temperature evolution on pion gas with second order theory have already been done in Ref. [15].

V. CONCLUSIONS

In the present article the third order shear relaxation equation in the Bjorken scenario has been developed following the earlier second order calculation by Muronga. In comparison to other third order models in similar scaling, solutions by El *et al.* and Jaiswal have been done. Consequently we have worked on checking the consistency of our calculations in a very simplistic scenario. This would serve as a test for future development into (3+1)D dissipative hydrodynamics. The differences in the results have been highlighted and discussed. The coupling coefficients in the relaxation equations from these models have been found to be slightly different from our calculations and the output is found to be sensitive to values of the coefficients. The difference also indicates one of the possible sources of uncertainties in the output and thus must be precisely evaluated. More detailed investigations on the effects of the coefficients on thermodynamic variables are being carried out. A comparison with the transport theory of BAMPS has been carried out via the P_L/P_T ratio plot. The BAMPS data have a similar trend to the results from the AM model. However the present method of using Grad's 14 moment approximation shows a considerable difference with transport results especially at high η/s values. This should be investigated and reported in the future. Nonlinear terms such as $\partial_i S_3^2$ and $\partial_i S_3^3$ associated with shear viscous

pressure have been included in the relaxation equation and have shown effects on the calculated thermodynamic quantities at low τ or for higher η/s values. However, because of the absence of coupling coefficients associated with other fluxes or correlated terms, the final outcome on the observed thermodynamic quantities is not conclusive. The assumptions are being relaxed and the precise determination of the coupling coefficients S_n^m and effect of EoS on them are being currently studied and will be reported soon. The third order correction to shear relaxation time τ_π has explicit effects of shear pressure π which was absent in the second order. Also the third order relaxation time $\tau_\pi^{(3)}$ is more than τ_π but appears to converge to it at later time. It would be interesting to study what effects ordered theories higher than 3 would bring on the relaxation time.

The ratio of longitudinal pressure to transverse pressure ratio calculated for $\eta/s > 0.5$ shows an almost flat and horizontal trend with time. This might indicate that system with high viscosity may not go back to equilibrium during a QGP lifetime. Consequently a detailed study of time-scale or system length-scale dependence of the relaxation time of dissipative fluxes and the correlation between the thermodynamic variables and transport coefficients could be carried out. This would also bring out in-depth information on ordered theories and correlation between system evolution, hadronization, and freeze-out times and various coupling coefficients. A precise determination of transport coefficients such as shear η and bulk ζ viscosities and thermal conductivity κ must also be carried out. Parton cascade and transport models like UrQMD, BAMPS, VNI/BMS, etc., could help us in the study. The study of time evolution of thermodynamic variables and transport coefficients would also help us develop the equation of state (EoS) which is vital for transport simulation [53–63].

It is also seen from first order theory, that there is a large increase in temperature and entropy production. They are almost an order in magnitude different from the ideal equation results. Both second and third order theories bring down this difference. As mentioned in Ref. [39], it would be also an interesting study to go beyond third order in present calculations to study the oscillatory nature of ordered theories on thermodynamic variables. Calculations needed to be done with full transport theories which include dissipative heat flow and bulk viscous pressure along with shear pressure and extend our theories to full dissipative hydrodynamics. One needs to study the changes in variables due to the additional effects of heat flow and bulk viscous pressure. Inclusion of bulk viscosity becomes important for the heavy ion collision systems with massive particles, large chemical potential, or other small systems from proton-proton collisions. Also our current study has been carried out for a single initial temperature of 500 MeV. Other values for initial temperature could be included to further elucidate temperature dependences of dissipative fluxes, entropy production, etc. Hadron medium effects were not included in this simple model. Works are being carried out although some results for the hadronic regime using second order theories have already been shown by Muronga *et al.* [15]. One of the many purposes of determining hydrodynamic attractors is to test the convergence of hydrodynamics coefficients to an arbitrary high order. It

shows the viability and applicability of the present form of relativistic fluid mechanics we are using today. The techniques could be extended to both massless and massive particles. A part of the current work could also be directed along the study of attractors in the near future.

ACKNOWLEDGMENTS

One of the authors (M.Y.) wishes to acknowledge the support of the Department of Physics, Nelson Mandela University in allowing us its facilities for the work. The author (M.Y.) is grateful to Research Capacity Development, Nelson Mandela University for supporting the project. The authors would like to thank Prof. Tomoi Koide for his valuable suggestions, and Dr. Amaresh Jaiswal for his valuable discussions on methods and providing us with BAMPS data from El *et al.*'s paper.

APPENDIX A

Some of the mathematical terms used in our calculations and shown in the paper have been explained here briefly. The deviation function $\phi(x)$ in Eq. (10) is written as a function of moments ϵ , ϵ_μ , and $\epsilon_{\mu\nu}$:

$$\phi(x) = \epsilon - \epsilon_\mu p^\mu + \epsilon_{\mu\nu} p^\mu p^\nu, \quad (\text{A1})$$

where the moments are function of dissipative fluxes as

$$\begin{aligned} \epsilon &= A_0, \\ \epsilon_\mu &= A_1 u_\mu \Pi - B_0 q_\mu, \\ \epsilon_{\mu\nu} &= A_2 (4u_\mu u_\nu - g_{\mu\nu}) \Pi - B_1 u_\mu q_\nu + C_0 \pi_{\mu\nu}. \end{aligned} \quad (\text{A2})$$

The coefficients in the moments in $\phi(x)$ are calculated to be

$$\begin{aligned} A_0 &= 3A_2 D_{20}^{-1} (D_{30} + I_{41} I_{20} - I_{30} I_{31}), \\ A_1 &= 3A_2 D_{20}^{-1} (4(I_{10} I_{41} - I_{20} I_{31})), \\ A_2 &= \frac{1}{4I_{42} \Omega}, \\ B_0 &= B_1 \frac{I_{41}}{I_{31}}, \\ B_1 &= \frac{1}{\Lambda I_{21}}, \\ C_0 &= \frac{1}{2I_{42}} \end{aligned} \quad (\text{A3})$$

with

$$\Lambda = \frac{D_{31}}{I_{21}^2} \quad (\text{A4})$$

and

$$\begin{aligned} \Omega &= -\frac{I_{10}}{D_{20} I_{31}} \left[I_{30} \left(I_{30} - \frac{I_{31}}{I_{21} I_{20}} \right) - I_{40} \left(I_{20} - \frac{I_{31}}{I_{21}} I_{10} \right) \right] \\ &\quad + \beta \frac{I_{41}}{I_{31}}. \end{aligned} \quad (\text{A5})$$

The integration I_{nk} is a scalar coefficient that depends on the equilibrium distribution parameters α and β . It appears in the

n th moment of the distribution function as (see Ref. [17])

$$\begin{aligned} I^{\mu_1 \dots \mu_n}(x) &= \int dw p_1^{\mu_1} \dots p_n^{\mu_n} f(x, p) \\ &= \sum_{k=0}^i a_{nk} I_{nk} \Delta^{(2k)} u^{n-2k}, \end{aligned} \quad (\text{A6})$$

where I_{nk} is given by

$$\begin{aligned} I_{nk} &= \frac{A_0}{(2k+1)!!} \int dw (p^\alpha u_\alpha - p^\alpha p_\alpha)^k (p^\mu u_\mu)^{n-2k} \\ &\quad \times \frac{1}{e^{\beta_\mu p^\mu - \alpha} - a}. \end{aligned} \quad (\text{A7})$$

The quantity, D_{nk} , can be shown to be

$$D_{nk} = I_{n+1,k} I_{n-1,k} - I_{n,k}^2. \quad (\text{A8})$$

In the ultrarelativistic limit, as rest mass $m \rightarrow 0$ with respect to a particles' kinetic energy, it can be shown that

$$I_{nk} = \frac{4\pi A_0}{(2k+1)!!} T^{n+2} \int_0^\infty dx x^{n+1} \frac{1}{e^{x-\phi}} \quad (\text{A9})$$

with $x = \frac{p}{T}$ and $z = \frac{m}{T}$ are the new variables. ϕ being the chemical potential has been taken to be zero here. Then we have

$$I_{nk} = \frac{4\pi A_0}{(2k+1)!!} T^{n+2} (n+1)!. \quad (\text{A10})$$

The quantities Ω that come in the bulk viscosity and Λ that appears in the thermal conductivity coefficient can now be reduced to

$$\Omega = 0, \quad \Lambda = 4T^2. \quad (\text{A11})$$

Using Eqs. (18)–(20), the coefficients for the second order in the entropy four-current, Eq. (21) have been calculated as

$$\begin{aligned} S_1^2 &= \frac{3}{\beta I_{42}^2 \Omega^2} \left(5I_{52} - \frac{3}{D_{20}} [I_{31} (I_{31} I_{30} - I_{41} I_{20}) \right. \\ &\quad \left. + I_{41} (I_{41} I_{10} - I_{31} I_{20})] \right), \\ S_2^2 &= \frac{D_{41}}{\beta \Lambda I_{21}^2 I_{31}}, \\ S_3^2 &= \frac{1}{2} \frac{I_{52}}{\beta I_{42}^2}, \\ S_4^2 &= \frac{D_{41} D_{20} - D_{31} D_{30}}{\beta \Lambda \Omega I_{42} I_{21} I_{31} D_{20}}, \\ S_5^2 &= \frac{I_{31} I_{52} - I_{41} I_{42}}{\beta \Lambda I_{42} I_{21} I_{31}}. \end{aligned} \quad (\text{A12})$$

The coefficients for the third order dissipative quantities in the entropy four-current, Eq. (21), have similarly been calculated as

$$\begin{aligned} S_1^3 &= \frac{1}{\beta} [I_{10} A_0^3 - 3I_{20} A_0^2 A_1 + 9I_{30} A_0^2 A_2 \\ &\quad - I_{40} A_1 (A_1^2 + 18A_0 A_2) + 9I_{50} A_2 (3A_0 A_2 - A_1^2) \\ &\quad - 27I_{60} A_1 A_2^2 + 27I_{70} A_2^3], \end{aligned}$$

$$\begin{aligned}
S_2^3 &= -\frac{1}{\beta} [3I_{41}B_0(2A_0B_1 + A_1B_0) + 3I_{51}(2A_1B_0B_1 - A_0B_1^2 \\
&\quad + 3A_2B_0^2) + 3I_{61}(6A_2B_0B_1 + A_1B_1^2) - 9I_{71}A_2B_1^2], \\
S_3^3 &= \frac{1}{\beta} [6I_{52}A_0C_0^2 - 6I_{62}A_1C_0^2 + 18I_{72}A_2C_0^2], \\
S_4^3 &= \frac{3C_0}{\beta} [I_{52}B_0^2 - 2I_{62}B_0B_1 + I_{72}B_1^2], \\
S_5^3 &= \frac{2I_{73}C_0^3}{\beta}, \\
S_6^3 &= \frac{3}{\beta} [I_{21}A_0^2B_0 + I_{31}A_0^2B_1 + I_{41}(A_1^2B_0 + 2A_0A_1B_1 \\
&\quad + 6A_0A_2B_1) + I_{51}(A_1^2B_1 - 6A_0A_2B_1 + 6A_1A_2B_0) \\
&\quad + 3I_{61}A_2(2A_1B_1 + 3A_2B_0) - 9I_{71}A_2^2B_1], \\
S_7^3 &= -\frac{1}{\beta} [I_{42}B_0^3 - 3I_{52}B_0^2B_1 + 3I_{62}B_0B_1^2 - I_{72}B_1^3], \\
S_8^3 &= \frac{3}{\beta} [I_{73}B_1C_0^2 - I_{63}B_0C_0^2], \\
S_9^3 &= -\frac{1}{\beta} [I_{42}A_0B_0C_0 - I_{52}A_1B_0C_0 + I_{52}A_0B_1C_0 \\
&\quad + I_{62}A_1B_1C_0 + 3I_{62}A_2B_0C_0 - 3I_{72}A_2B_1C_0], \\
S_{10}^3 &= \frac{1}{\beta} [I_{73}B_1C_0^2 - I_{63}B_0C_0^2]. \tag{A13}
\end{aligned}$$

In the ultra-relativistic limits, the coefficients can be shown to be, e.g.,

$$\begin{aligned}
\Lambda &\rightarrow \frac{1}{2}P^{-1}, \quad S_2^2 \rightarrow \frac{5}{4}P^{-1}, \quad S_3^2 \rightarrow \frac{3}{4}P^{-1}, \\
S_5^2 &\rightarrow \frac{1}{7}P^{-1}, \quad S_4^3 \rightarrow 6P^{-2}, \quad S_5^3 \rightarrow \frac{3}{4}P^{-2}, \\
S_7^3 &\rightarrow 2P^{-2}, \quad S_{10}^3 \rightarrow \frac{1}{32}P^{-2}, \quad \text{etc.},
\end{aligned}$$

$$\text{where } P = I_{21} = \frac{4\pi A_0}{3} T^4 3! \quad \text{is the pressure.}$$

(A14)

APPENDIX B

Using the entropy principle $\partial_\mu S^\mu \geq 0$ and Eq. (21) the third order expression for the dissipative fluxes been calculated as

$$\begin{aligned}
\Pi &= -\zeta [\nabla_\alpha u^\alpha + 2S_2^2 \dot{\Pi} + S_4^2 \nabla_\alpha q^\alpha + \Pi(S_1^2 + S_1^2 \nabla_\alpha u^\alpha) \\
&\quad + q^\alpha (\nabla_\alpha S_4^2 - S_4^2 \dot{u}^\alpha) + 3S_1^3 \dot{\Pi} \Pi + 2S_2^3 \dot{q}_\alpha q^\alpha
\end{aligned}$$

$$\begin{aligned}
&+ 2S_3^3 \dot{\pi}_{(\alpha\beta)} \pi^{(\alpha\beta)} + S_6^3 (\Pi \nabla_\alpha q^\alpha + q^\alpha \nabla_\alpha \Pi) \\
&+ S_9^3 (\pi^{(\alpha\beta)} \nabla_\alpha q_\beta + q_\beta \nabla_\alpha \pi^{(\alpha\beta)}) \\
&+ \Pi^2 (\dot{S}_1^3 + S_1^3 \nabla_\alpha u^\alpha) - q^\alpha q_\alpha (\dot{S}_2^3 + S_2^3 \nabla_\alpha u^\alpha) \\
&+ \pi^{2(\alpha\beta)} (\dot{S}_3^3 + S_3^3 \nabla_\alpha u^\alpha) + \Pi q^\alpha (\nabla_\alpha S_6^3 - S_6^3 \dot{u}_\alpha) \\
&+ \pi^{(\alpha\beta)} q_\beta (\nabla_\alpha S_9^3 - S_9^3 \dot{u}_\alpha), \tag{B1}
\end{aligned}$$

$$\begin{aligned}
q^\alpha &= \kappa T \Delta^{\alpha\mu} \left[\left(\frac{\nabla_\alpha T}{T} - \dot{u}_\alpha \right) + 2S_2^2 \dot{q}_\alpha + S_4^2 \nabla_\alpha \Pi \right. \\
&+ S_5^2 \nabla^\beta \pi_{(\alpha\beta)} + q_\alpha (\dot{S}_2^2 + S_2^2 \nabla_\nu u^\nu) + \Pi (\nabla_\alpha S_4^2 - S_4^2 \dot{u}_\alpha) \\
&+ \pi_{(\alpha\beta)} (\nabla^\beta S_5^2 - S_5^2 \dot{u}^\beta) - S_2^3 (2\Pi \dot{q}_\alpha + q_\alpha \dot{\Pi}) \\
&+ S_4^3 (2q^\beta \pi_{(\alpha\beta)} + q^\beta \dot{\pi}_{(\alpha\beta)}) + 2S_6^3 \Pi \nabla_\alpha \Pi \\
&- 2S_7^3 q^\beta \nabla_{q_\beta} + S_9^3 (\Pi \nabla^\beta \pi_{(\alpha\beta)} + \pi_{(\alpha\beta)} \nabla^\beta \Pi) \\
&+ 2S_{10}^3 \pi_{(\beta\nu)} \nabla_\alpha \pi^{(\alpha\nu)} - \Pi q_\alpha (\dot{S}_2^3 + S_2^3 \nabla_\nu u^\nu) \\
&+ q^\beta \pi_{(\alpha\beta)} (S_4^3 + S_4^3 \nabla_\nu u^\nu) + \Pi^2 \nabla_\alpha S_6^3 \\
&- q^\lambda q_\lambda \nabla_\alpha S_7^3 + \pi^{2(\lambda\lambda)} \nabla_\alpha S_8^3 + 2S_8^3 \pi^{(\mu\nu)} \nabla_\alpha \pi_{(\mu\nu)} \\
&+ \Pi \pi_{(\alpha\beta)} (\nabla^\beta S_9^3 - S_9^3 \dot{u}^\beta) + \pi_{(\alpha\beta)}^2 (\nabla^\beta S_{10}^3 - S_{10}^3 \dot{u}^\beta) \\
&\left. + S_7^2 q_\alpha q^\lambda q_\lambda \right], \tag{B2}
\end{aligned}$$

$$\begin{aligned}
\pi^{(\mu\nu)} &= 2\eta \Delta^{\alpha\mu} \Delta^{\beta\nu} [\nabla_\alpha u_\beta + 2S_2^2 \pi_{(\alpha\beta)} \\
&+ S_5^2 \nabla_{(\alpha} q_{\beta)} + \pi_{(\alpha\beta)} (\dot{S}_3^2 + S_3^2 \nabla_\lambda u^\lambda) \\
&+ q_\alpha (\nabla_\beta S_5^2 - S_5^2 \dot{u}_\beta) + S_3^3 (2\Pi \dot{\pi}_{(\alpha\beta)} + \pi_{(\alpha\beta)} \dot{\Pi}) \\
&+ 2S_4^3 \dot{q}_{(\alpha} q_{\beta)} + 3S_5^3 \dot{\pi}_{(\alpha\lambda)} \pi_{\beta)}^\lambda + S_8^3 \pi_{(\alpha\beta)} \nabla_\lambda u^\lambda \\
&+ S_9^3 (\Pi \nabla_{(\alpha} q_{\beta)} + q_{(\alpha} \nabla_{\beta)} \Pi) + S_{10}^3 (q_{(\alpha} \nabla^\lambda \pi_{(\alpha)\lambda)} \\
&+ \pi_{(\lambda(\alpha)} \nabla^\lambda q_{\beta)} + \Pi \pi_{(\alpha\beta)} (\dot{S}_3^3 + S_3^3 \nabla_\lambda u^\lambda) \\
&+ q_{(\alpha} q_{\beta)} (\dot{S}_4^3 + S_4^3 \nabla_\lambda u^\lambda + \pi_{(\alpha\lambda)} \pi_{\beta)}^\lambda (S_5^3 + S_5^3 \nabla_\lambda u^\lambda) \\
&+ \pi_{(\alpha\beta)} q^\lambda (\nabla_\lambda S_8^3 - S_8^3 \dot{u}_\lambda) + \Pi q_{(\alpha} (\nabla_{\beta)} S_9^3 - S_9^3 \dot{u}_{\beta)}) \\
&\left. + \pi_{(\alpha\lambda)} q^\lambda (\nabla_{\beta)} S_{10}^3 - S_{10}^3 \dot{u}_{\beta)}) \right]. \tag{B3}
\end{aligned}$$

Thus up to third order the bulk, heat, and shear equations are the sum of the zeroth, first, second, and third order contributions.

- [1] J. W. Harris and B. Muller, *Annu. Rev. Nucl. Part. Sci.* **46**, 71 (1996).
[2] S. S. Adler *et al.* (PHENIX Collaboration), *Phys. Rev. Lett.* **91**, 182301 (2003).

- [3] Q. Li, C. Shen, and M. Bleicher, *Centr. Eur. J. Phys.* **10**, 1131 (2012).
[4] B. B. Abelev *et al.* (ALICE Collaboration), *J. High Energy Phys.* **06** (2015) 190.

- [5] H. Stoecker and W. Greiner, *Phys. Rep.* **137**, 277 (1986).
- [6] S. A. Bass, M. Gyulassy, H. Stoecker, and W. Greiner, *J. Phys. G* **25**, R1 (1999).
- [7] M. Bleicher *et al.*, *J. Phys. G* **25**, 1859 (1999).
- [8] J. I. Kapusta, *Phys. Rept.* **88**, 365 (1982).
- [9] C. Eckart, *Phys. Rev.* **58**, 919 (1940).
- [10] L. D. Landau and E. M. Lifshitz, *Fluid Mechanics* (Pergamon, New York, 1959).
- [11] I. Muller, *Z. Phys.* **198**, 329 (1967).
- [12] W. Israel, *Ann. Phys. (NY)* **100**, 310 (1976).
- [13] J. M. Stewart, *Proc. R. Soc. Lond. A* **357**, 59 (1977); W. Israel and J. M. Stewart, *Ann. Phys. (NY)* **118**, 341 (1979).
- [14] A. Muronga, *Phys. Rev. Lett.* **88**, 062302 (2002); **89**, 159901(E) (2002).
- [15] A. Muronga, *Phys. Rev. C* **69**, 034903 (2004).
- [16] A. Muronga, *Phys. Rev. C* **76**, 014909 (2007).
- [17] A. Muronga, *Phys. Rev. C* **76**, 014910 (2007).
- [18] A. El, A. Muronga, Z. Xu, and C. Greiner, *Phys. Rev. C* **79**, 044914 (2009).
- [19] A. El, A. Muronga, Z. Xu, and C. Greiner, *Nucl. Phys. A* **848**, 428 (2010).
- [20] G. S. Denicol, T. Koide, and D. H. Rischke, *Phys. Rev. Lett.* **105**, 162501 (2010).
- [21] A. Jaiswal, *Phys. Rev. C* **87**, 051901(R) (2013).
- [22] A. Jaiswal, B. Friman, and K. Redlich, *Phys. Lett. B* **751**, 548 (2015).
- [23] R. S. Bhalerao, A. Jaiswal, S. Pal, and V. Sreekanth, *Phys. Rev. C* **89**, 054903 (2014).
- [24] M. Attems, Y. Bea, J. Casalderrey-Solana, D. Mateos, M. Triana, and M. Zilhao, *J. High Energy Phys.* **06** (2017) 129.
- [25] A. Jaiswal and V. Roy, *Adv. High Energy Phys.* **2016**, 9623034 (2016).
- [26] H. Saida, [arXiv:1705.05521](https://arxiv.org/abs/1705.05521) [gr-qc].
- [27] F. S. Bemfica, M. M. Disconzi, and J. Noronha, *Phys. Rev. Lett.* **122**, 221602 (2019).
- [28] R. Ryblewski, *J. Phys. Conf. Ser.* **612**, 012058 (2015).
- [29] M. P. Heller, R. A. Janik, and P. Witaszczyk, *Phys. Rev. Lett.* **110**, 211602 (2013).
- [30] S. Grozdanov and N. Kaplis, *Phys. Rev. D* **93**, 066012 (2016).
- [31] R. Baier, P. Romatschke, D. T. Son, A. O. Starinets, and M. A. Stephanov, *J. High Energy Phys.* **04** (2008) 100.
- [32] S. Jaiswal, C. Chattopadhyay, A. Jaiswal, S. Pal, and U. Heinz, *Phys. Rev. C* **100**, 034901 (2019).
- [33] A. Muronga, *J. Phys. G* **37**, 094008 (2010).
- [34] J. Y. Ollitrault, *Eur. J. Phys.* **29**, 275 (2008).
- [35] A. Sinha and R. C. Myers, *Nucl. Phys. A* **830**, 295c (2009).
- [36] J. D. Bjorken, *Phys. Rev. D* **27**, 140 (1983).
- [37] H. Grad, *Commun. Pure Appl. Math* **2**, 331 (1949).
- [38] W. A. Hiscock and L. Lindblom, *Ann. Phys. (NY)* **151**, 466 (1983).
- [39] A. El, Z. Xu, and C. Greiner, *Phys. Rev. C* **81**, 041901(R) (2010).
- [40] A. Jaiswal, *Phys. Rev. C* **88**, 021903(R) (2013).
- [41] A. Jaiswal, *Nucl. Phys. A* **931**, 1205 (2014).
- [42] P. Romatschke and U. Romatschke, [arXiv:1712.05815](https://arxiv.org/abs/1712.05815) [nucl-th].
- [43] M. O-Starzewski, *Int. J. Eng. Sc.* **47**, 807 (2009).
- [44] B. Betz, D. Henkel, and D. H. Rischke, *J. Phys. G* **36**, 064029 (2009).
- [45] T. Koide, G. S. Denicol, P. Mota, and T. Kodama, *Phys. Rev. C* **75**, 034909 (2007).
- [46] G. Baym, H. Monien, C. J. Pethick, and D. G. Ravenhall, *Phys. Rev. Lett.* **64**, 1867 (1990).
- [47] G. Baym and H. Heiselberg, *Phys. Rev. D* **56**, 5254 (1997).
- [48] Y. Aoki, S. Borsanyi, S. Durr, Z. Fodor, S. D. Katz, S. Krieg, and K. K. Szabo, *J. High Energy Phys.* **06** (2009) 088.
- [49] Y. Aoki, S. Borsanyi, S. Durr, Z. Fodor, S. D. Katz, S. Krieg, and K. K. Szabo, *Nucl. Phys. A* **830**, 805c (2009).
- [50] R. C. Hwa and K. Kajantie, *Phys. Rev. D* **32**, 1109 (1985).
- [51] D. K. Srivastava, C. Gale, and R. J. Fries, *Phys. Rev. C* **67**, 034903 (2003).
- [52] J. Adam *et al.* (ALICE Collaboration), *Phys. Rev. Lett.* **116**, 222302 (2016).
- [53] B. Zhang, M. Gyulassy, and Y. Pang, *Phys. Rev. C* **58**, 1175 (1998).
- [54] D. Pal, B. K. Patra, and D. K. Srivastava, *Eur. Phys. J. C* **17**, 179 (2000).
- [55] S. A. Bass, B. Muller, and D. K. Srivastava, *Phys. Lett. B* **551**, 277 (2003).
- [56] A. Muronga, *J. Phys. G* **35**, 044073 (2008).
- [57] S. De, D. K. Srivastava, and R. Chatterjee, *J. Phys. G* **37**, 115004 (2010).
- [58] J. Fuini III, N. S. Demir, D. K. Srivastava, and S. A. Bass, *J. Phys. G* **38**, 015004 (2011).
- [59] A. Muronga, *Phys. Rev. C* **69**, 044901 (2004).
- [60] Z. Xu and C. Greiner, *Phys. Rev. C* **71**, 064901 (2005).
- [61] Z. Xu and C. Greiner, *Phys. Rev. Lett.* **100**, 172301 (2008).
- [62] C. Wesp, A. El, F. Reining, Z. Xu, I. Bouras, and C. Greiner, *Phys. Rev. C* **84**, 054911 (2011).
- [63] Z. Chen, C. Greiner, Z. Xu, and P. Zhuang, *Phys. Rev. C* **100**, 014906 (2019).